Journal of Materials Chemistry C

RSC Publishing

PAPER

View Article Online
View Journal | View Issue

Charge transfer relaxation in donor–acceptor type conjugated materials†

Cite this: *J. Mater. Chem. C*, 2013, **1**, 2308

Mariateresa Scarongella,[a] Andrey Laktionov,[b] Ursula Rothlisberger[b] and Natalie Banerji*[a]

Received 11th December 2012
Accepted 20th January 2013

DOI: 10.1039/c3tc00829k

www.rsc.org/MaterialsC

The development of conjugated materials bearing electron-rich and electron-poor units along their backbone introduces new possibilities to control functionality for organic electronic applications through charge transfer character in ground and excited states. A thorough understanding of intramolecular dipoles and their evolution during excited state relaxation is necessary in order to fully exploit this opportunity. PCDTBT is an alternating donor–acceptor copolymer with high photovoltaic efficiency in bulk heterojunction solar cells. We use time-resolved femtosecond transient absorption spectroscopy in solution and in the solid state to study PCDTBT and the dTBT and CDTBT model compounds, fragments of the polymer chain. Higher solubility and slower relaxation make CDTBT particularly suitable to understand the mechanism of charge transfer relaxation in this class of materials. A progressive increase of charge transfer character from the initially moderately polar excited state is mainly driven by solvent reorganization and some torsional rearrangements. Similar relaxation in solid state CDTBT might ultimately lead to the formation of separate charges.

1 Introduction

Conjugated polymers are successful organic electronic materials.[1–5] Their functioning is often based on processes that occur in the excited state, populated either by optical absorption in organic photovoltaic (OPV) systems[6–10] or by electrical stimuli in organic light-emitting diodes (OLEDs).[11–15] These processes can be extremely fast. For example, the key step for photocurrent generation in solar cells, charge separation in photoexcited polymer:fullerene blends, has sub-100 femtosecond (fs) components.[16–19] The functional processes can therefore compete with or be driven by fast excited state relaxation, *i.e.* cooling and conformational/electronic response of the material after being promoted to higher energy. When designing new materials and devices, it is therefore extremely important to understand this relaxation and to account for its effects on the wanted phenomena. Although relaxation in conjugated molecules has been intensely investigated,[20–26] the implication on device functioning has only been little discussed.[27–30]

A popular way to lower the bandgap of OPV materials for better light harvesting or to induce ambipolar charge transport in field effect transistors is to alternate electron-donating and electron-withdrawing groups along the conjugated polymer backbone (donor–acceptor approach).[7,31–35] This introduces the possibility of dipole moments in the ground and excited states, as well as for change in this intramolecular charge transfer (ICT) character during relaxation. PCDTBT attracted attention in 2009 as the first donor–acceptor copolymer with high OPV power conversion efficiency exceeding 6% (today, 7.2% can be achieved with this material).[8,36–38] We have previously investigated relaxation in dissolved and thin film PCDTBT by time-resolved fluorescence spectroscopy and noted effects occurring on the <200 fs time scale.[30] For conjugated polymers in general, the observed <200 fs red shift of the emission spectrum and loss of polarization memory are ascribed to complex electronic and conformational changes leading to dynamic localization of the excited state.[24,25,39–41] Scholes *et al.* have recently shown using two-dimensional electronic spectroscopy that for PCDTBT there is additionally an increase in the excited state charge transfer character during ultrafast relaxation.[20] This significant phenomenon is however difficult to investigate in detail and using more conventional techniques, because of the limited polymer solubility (preventing solvent-dependent studies) and the experimentally rather inaccessible ~200 fs time scale.

We present here a strategy to study charge transfer relaxation of PCDTBT using the oligomeric model compounds dTBT and CDTBT (Fig. 1), thus fragments of the polymer chain. Both contain the benzothiadiazole (BT) electron-withdrawing unit and either thiophenes or both thiophene and carbazole electron-donating units, so that they can be considered as

[a]*Photochemical Dynamics Group, Institute of Chemical Sciences and Engineering, Ecole Polytechnique Fédérale de Lausanne, CH-1015 Lausanne, Switzerland. E-mail: natalie.banerji@epfl.ch*

[b]*Laboratory of Computational Chemistry and Biochemistry, Institute of Chemical Sciences and Engineering, Ecole Polytechnique Fédérale de Lausanne, CH-1015 Lausanne, Switzerland*

† Electronic supplementary information (ESI) available: Additional figures, tables and computational results, as mentioned in the text. See DOI: 10.1039/c3tc00829k

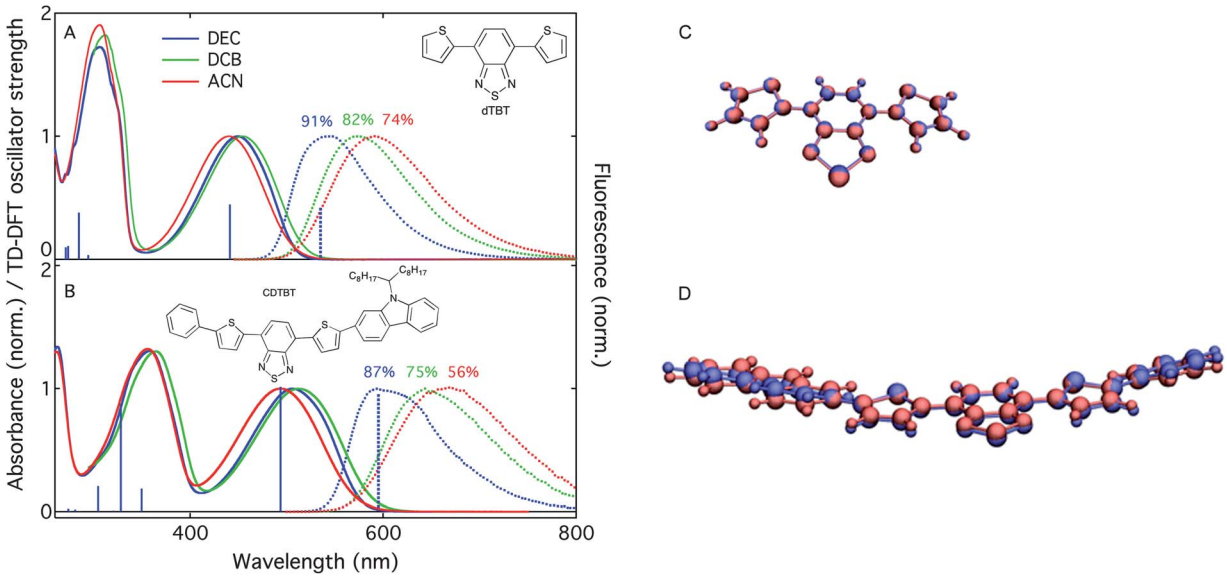

Fig. 1 Steady-state absorption and emission spectra of dTBT (A) and CDTBT (B) in various solvents, together with the fluorescence quantum yields and the gas-phase transitions calculated by TD-DFT (M062X/6-31+G*, solid and dashed vertical blue lines for absorption and emission). Optimized geometries of dTBT (C) and CDTBT (D) in the ground state in blue and in the relaxed emitting state in red, obtained from the calculations.

donor–acceptor type conjugated materials. We have previously reported for the first time the synthesis of CDTBT and used the breakdown of the PCDTBT polymer into its building blocks to elucidate its electronic structure through steady-state experimental techniques and DFT calculations.[42] Now, we have used time-resolved femtosecond transient absorption (TA) spectroscopy to understand excited state relaxation of dTBT, CDTBT and PCDTBT.

We identify CDTBT as an excellent system to study the mechanism of charge transfer relaxation in this class of materials. The S_1 state with initially moderate ICT character is populated by direct excitation in the first absorption band or *via* ultrafast internal conversion (<200 fs) following excitation in the second band. In polar solvents only, relaxation involving mainly intermolecular solvation and some intramolecular planarization then stabilizes a form with stronger ICT character and reduced emission quantum yield. We could directly follow this charge transfer relaxation, which also occurs in solid state thin films where neighboring molecules replace the solvent. In this case, there is evidence that intermolecular interactions might subsequently lead to formation of separate charges. At the end of the manuscript, we examine the importance of charge transfer character and relaxation in conjugated donor–acceptor materials for device applications.

2 Experimental methods

2.1 Samples

The dTBT (4,7-di-(2-thienyl)-2,1,3-benzothiadiazole) and CDTBT (4-(5-(*N*-(9-heptadecanyl)carbazol-2-yl)thiophen-2-yl)-7-(5-phenylthiophen-2-yl)benzo[2,1,3]thiadiazole) materials were synthesized as previously described.[42,43] The latter was recrystallized from acetone prior to the measurements to ensure highest purity. PCDTBT (poly[*N*-9′′-hepta-decanyl-2,7-carbazole-alt-5,5-(4′,7′-di-2-thienyl-2′,1′,3′-benzothiadiazole)]) was synthesized by St-Jean Photochimie Inc. (M_n = 39 000, M_w = 104 000, PDI = 2.7), according to the method reported elsewhere.[37,38] The solvents used were of highest available commercial purity. The CDTBT thin film was drop cast from a dichlorobenzene–chloroform mixture onto a sapphire substrate.

2.2 Steady-state measurements

Absorption spectra were recorded on a PerkinElmer Lambda 950 spectrophotometer in a 1 cm cell. No spectral changes with concentration were observed in the used range; so aggregation effects can be excluded. The fluorescence emission spectra were obtained in 90° configuration on a Horiba Jobin Yvon Fluorolog (FL-1065) with solutions that absorbed less than 0.05 in the visible range. The fluorescence quantum yield of dTBT was determined against perylene in acetonitrile ($\Phi_{fl} = 0.87$) (ref. 44) at 440 nm. For CDTBT, rhodamine 6G ($\Phi_{fl} = 0.99$) (ref. 45) was the reference with 480 nm excitation. The following equation was used:

$$\Phi_f = \frac{\int F(\lambda)}{\int F_{ref}(\lambda)} \cdot \left(\frac{n}{n_{ref}}\right) \cdot \frac{1 - 10^{A_{ref}}}{1 - 10^{A}} \cdot \Phi_{ref}$$

Here, $\int F(\lambda)$ represents the integral of the sample fluorescence spectrum, n is the refractive index of the solvent and A is the absorbance at the excitation wavelength. The quantities indexed as ref concern the reference standard solution.

2.3 Transient absorption spectroscopy

Transient absorption spectra were recorded using femtosecond pulsed laser pump-probe spectroscopy. Solutions were

measured in a 1 mm cell (0.2–0.3 absorbance at the excitation wavelength, or lower for solubility reasons), and constantly bubbled with an inert gas to provide stirring and to remove oxygen. The CDTBT thin film (~0.6 absorbance) was measured in a chamber that had been sealed inside a glovebox. For 490 nm, 510 nm or 530 nm excitation, the pump beam was generated with a commercial two-stage non-collinear optical parametric amplifier (NOPA-Clark, MXR) from the 780 nm output of a Ti:sapphire laser system with a regenerative amplifier providing 170 fs pulses at a repetition rate of 1 kHz. Compression of the NOPA output with two prisms lead to a 60 fs pulse duration. The pump power at the sample was 0.9–1.0 mW in solution and 0.5 mW (or 0.25 mW) for the thin film with a beam diameter of about 850 μm (determined with a BC106-Vis Thorlabs beam profiler). This corresponds to fluences of 160 μJ cm^{-2} and 90 μJ cm^{-2} (45 μJ cm^{-2}) in solution and film, respectively. For 390 nm excitation, the output of the Ti:sapphire laser was frequency doubled and similar fluences were used. For the small molecule building blocks in solution, chromophores are sufficiently separated so that excited state annihilation effects are not expected at the used excitation intensity. The linearity of the TA response was also verified by comparison to lower fluence data. For the multichromophoric polymer and solid state samples, fluence effects are discussed in the text.

The probe consisted of a white light continuum (420–950 nm), generated by passing a portion of the 780 nm amplified Ti:sapphire output through a c-cut 3 mm thick sapphire plate. Either a 750 nm low pass or a 850 nm high pass filter was used to remove the remaining fundamental intensity from the white light. The visible and n-IR parts of the spectrum were thus recorded separately (and sometimes had to be scaled to match in intensity). The probe intensity was always less than the pump intensity and the spot size was much smaller. The probe pulses were time delayed with respect to the pump pulses using a computerized translation stage. The probe beam was split before the sample into a signal beam (transmitted through the sample and crossed with the pump) and a reference beam. The signal and reference beams were detected with a pair of 163 mm spectrographs (Andor Technology, SR163) equipped with a 512 × 58 pixel back-thinned CCD (Hamamatsu S07030-0906) and assembled by Entwicklungsbüro Stresing, Berlin. To improve sensitivity, the pump light was chopped at half the amplifier frequency, and the transmitted signal intensity was recorded shot by shot. It was corrected for intensity fluctuations using the reference beam. The transient spectra were averaged until the desired signal-to-noise ratio was achieved (3000 times). The polarization of the probe pulses was at the magic angle relative to that of the pump pulses. All spectra were corrected for the chirp of the white-light probe.

2.4 Computational details

We performed the calculation of the electronic absorption and emission spectra for the dTBT and CDTBT molecules in the gas phase by means of Time-Dependent Density Functional Theory (TD-DFT),[46,47] in the adiabatic approximation,[48] using the M062X functional and 6-31+G* basis set.[49] Ground state geometries of dTBT and CDTBT had been previously optimized at the DFT level with B3LYP/6-31G**.[42] All calculations were performed with Gaussian09.[50] Molecular orbitals were visualized using VMD-1.9.[51]

3 Results and discussion

3.1 Steady-state transitions

The steady-state absorption and emission spectra of dTBT and CDTBT are shown in Fig. 1 for solvents of increasing polarity: decane (DEC, $\varepsilon = 2.0$), *o*-dichlorobenzene (DCB, $\varepsilon = 10.1$) and acetonitrile (ACN, $\varepsilon = 36.6$). Both molecules have two broad absorption bands in the shown range, with maxima that do not correlate with solvent polarity but, as we have shown previously,[42] with the refractive index. The negligible polarity dependence points to a very small dipole moment in the ground state and/or very moderate or absent charge transfer during the involved transitions. The former effect might be more predominant, given that our previous TD-DFT calculations using B3LYP/6-31G** suggest partial redistribution of electron density toward the BT electron accepting unit in both materials during absorption in both bands (with weaker ICT character and more delocalization in the second band).[42] A B3LYP computation of a larger tetrameric polymer segment by Brédas *et al.* indicates similar transitions in PCDTBT,[52] but later the same authors found that ICT character is exaggerated with this method.[53] In general, it must be borne in mind that DFT calculations are limited by approximations used in the underlying functionals (especially exchange-correlation); so the delocalization of the wavefunctions is often exaggerated and charge transfer transitions are difficult to describe. To overcome these limitations, specialized functionals (such as long range-separated ones) can be used and must be chosen appropriately for the investigated material. Moreover, purely electronic transitions are typically calculated by TD-DFT (no vibrational coupling), in the gas phase (no solvent environment) and at 0 K (no conformational disorder), so that small shifts compared to the experiment are expected even if the used functional is highly adapted for the studied system.

Here, we have repeated the gas-phase TD-DFT simulations for dTBT and CDTBT at the M062X/6-31+G* level of theory. This functional yields more accurate charge transfer excitation energies than B3LYP and is much more appropriate for transitions with low orbital overlap between the donor and acceptor regions.[54,55] The calculated transitions are best compared to experimental absorption data in non-polar DEC (low dielectric constant as in the gas phase). Fig. 1 reveals an excellent agreement between theory and experiment, much better than the underestimated transition energies previously obtained with B3LYP for both compounds and absorption bands. Nevertheless, the M062X results remain qualitatively similar to what we found in our initial B3LYP study, with only the $S_0 \rightarrow S_1$ transition in the first experimental absorption band and several transitions in the second one. Electron density differences for the M062X calculations between ground and excited states showing the electron/hole distributions for the $S_0 \rightarrow S_1$–S_3 transitions together with the corresponding projections into

Kohn–Sham one-particle orbitals are shown in Fig. S1 and S2 of the ESI.† The transitions in both bands have some concentration of electron density on the BT unit during absorption (partial ICT character). Also, the similarity of the calculated transitions in dTBT and CDTBT is in excellent agreement with the similar two broad bands in the experimental spectra. In contrast to our results with the oligomeric model systems, it has recently been suggested that the second absorption band in the PCDTBT polymer is localized on the carbazole and the adjacent thiophene segments, with no ICT and no contribution of the thiadiazole electron acceptor.[56] We are currently performing further calculations in order to understand this discrepancy. It does however not seem probable to us that the second absorption band in PCDTBT has a completely different origin than the second absorption band of the related CDTBT fragment, which (in view of the similarity with dTBT and the DFT calculations) clearly involves the thiadiazole.

The fluorescence spectra of dTBT and CDTBT behave very differently from the absorption spectra. The single emission band of both molecules becomes increasingly red shifted, broader and more symmetrical when more polar solvents are used, implying that the relaxed emitting state has pronounced ICT character and becomes stabilized in polar environments (Fig. 1). We have now also determined the fluorescence quantum yields, shown above the corresponding spectra in Fig. 1. The two materials are highly fluorescent in DEC, but the emission yield decreases with increasing solvent polarity. It is generally slightly lower in CDTBT than in dTBT and the decrease when going to ACN is more pronounced in CDTBT. This decrease is consistent with stabilization of partial charges, leading to a decreased overlap of the electron/hole distributions and hence to reduced oscillator strength of the transition. From a detailed solvatochromism study, we have previously estimated a higher dipole moment (10.1 Debye) in the emitting state of CDTBT compared to dTBT (5.7 Debye),[42] again in agreement with the trend in quantum yields. We note that the relatively high emission for both compounds in solution (even ACN) confirms partial charge transfer in the relaxed excited state, not formation of separate charges.

3.2 Charge transfer relaxation

3.2.1 CDTBT in solution (510 nm excitation). Time-resolved TA spectra of CDTBT dissolved in the three solvents and excited in the low energy band at 510 nm are shown in Fig. 2. The negative band in the 500 nm region is ascribed to the ground state bleach (GSB), based on its spectral coincidence with the first steady-state absorption band. The more red-shifted negative signature is due to stimulated emission (SE). Positive signatures of excited state absorption (ESA) are predominant above 700 nm, although they extend into the GSB/SE region, where the overlap is more visible in the polar solvents with weaker SE.

In DEC, the ESA is characterized by a sharp peak at 845 nm. There is hardly any evolution of the TA features on the investigated 1 ns time scale, except for some weak spectral dynamics. Global analysis of the TA time profiles (selected ones are shown in Fig. 2D) yields a 12 ps as well as a several nanosecond component due to the long-lived singlet excited state of CDTBT. The amplitude spectrum (from the pre-exponential factors) associated with the short 12 ps time constant reveals that there is a rise and narrowing of the positive 845 nm ESA band and a slight red shift of the SE obvious in the 600 nm region (Fig. 3A; note that a rise in the dynamics is characterized by the observed negative pre-exponential factor at certain wavelengths). We ascribe those spectral changes in the non-polar solvent to vibrational cooling and conformational relaxation.[44,57] The conformational relaxation of CDTBT in the gas phase

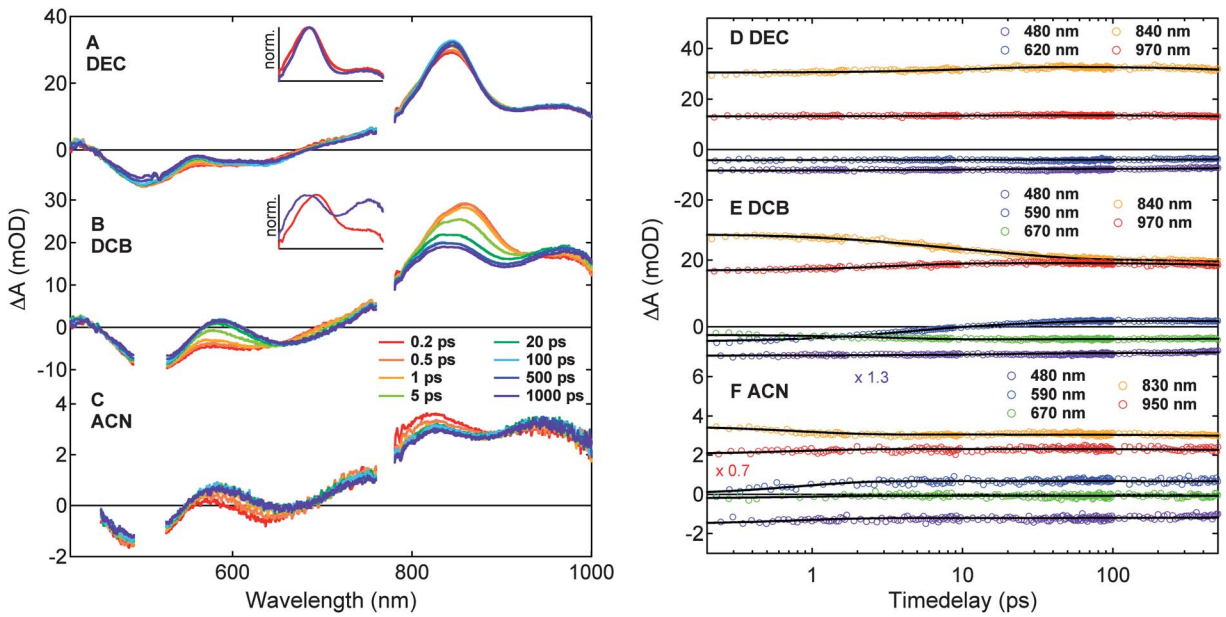

Fig. 2 Transient absorption spectra of CDTBT in different solvents, recorded at various time delays following excitation at 510 nm (A–C). Corresponding transient absorption dynamics at selected probe wavelengths (D–F). Solid lines represent the best multiexponential global fit.

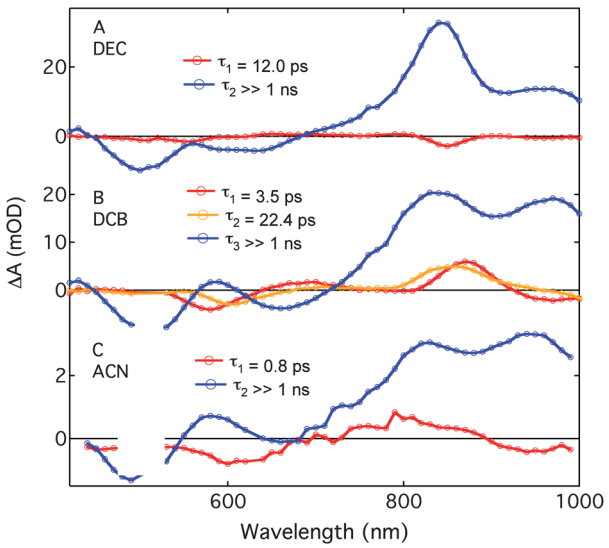

Fig. 3 Amplitude spectra associated with the time constants resulting from a multiexponential global analysis of the transient absorption dynamics of CDTBT in different solvents (510 nm excitation).

(comparable to non-polar DEC) was determined using TD-DFT/M06-2X geometry optimization in the excited state, leading to an excellent correspondence between the calculated and experimental emission spectra (Fig. 1B). It can be deduced that there is planarization of the CDTBT molecule in the relaxed excited state (Fig. 1D). In the ground state geometry, the thiophenes are rotated by about 15° with respect to the BT unit, while the dihedral angles between the thiophene and carbazole and between the thiophene and phenyl ring are around 29° (Figure S3†). Those angles respectively relax to ~0°, 16° and 20° in the emitting state.

The relaxation of the TA spectra of CDTBT in more polar DCB (Fig. 2B) is clearly very different. The early signature of the ESA resembles the one in DEC, except that the peak is at 860 nm. This peak then decays and shifts to 840 nm, although the persistence of the GSB and SE indicates that the system stays in an excited state. There is a concomitant red shift of the SE and rise of the 960 nm ESA shoulder, which is only little pronounced in DEC and in the early DCB spectra (see dynamics in Fig. 2E). The global analysis reveals that two time constants of 3.5 ps and 22.4 ps are associated with the relaxation processes causing the spectral changes (Fig. 3B). After about 100 ps, the TA features remain constant, with a double-peaked ESA signature that lives on the nanosecond time scale.

In polar solvents, a solvent reorganization around the molecule to accommodate the electronic redistribution in the excited state is to be expected, especially if the latter shows ICT character. This typically leads to a dynamic Stokes shift of the emission (a red shift as the excited state becomes stabilized).[58] The time scale of the spectral relaxation observed here for CDTBT in DCB is comparable to the multiphasic solvational time reported for aromatic molecules in benzene (0.2 ps, 1.9 ps and 24.7 ps).[58] The relaxation in CDTBT is therefore at least partially driven by solvation. The important changes in the ESA signature point however to a more complex mechanism with relaxation from the initially excited state with moderate charge transfer character (and a similar spectrum as in DEC) to a relaxed excited state with pronounced ICT character (not accessible in non-polar DEC), which we will for simplicity refer to as the "ICT form". This also perfectly explains the observed solvatochromism, *i.e.* dependence of only the emission and not absorption spectrum on solvent polarity. Such charge transfer relaxation is not uncommon in organic donor–acceptor dyads, and usually depends on both solvent and intramolecular coordinates.[44,59,60] While the ICT form is often characterized by an out-of-plane twist of the aromatic sub-units,[59] our TD-DFT results (Fig. 1D) suggest that the relaxed conformation in CDTBT is more planar than that in the ground or directly excited state. This is consistent with the planar intramolecular charge transfer (PICT) recently reported for covalent compounds also involving the BT, carbazole and related fluorine units.[61]

Based on the double-peaked ESA after relaxation for CDTBT in DCB (Fig. 2B), it cannot be excluded that both forms of the excited state (with more and less ICT character) coexist or are in equilibrium, possibly due to conformational disorder. The presence of the 960 nm shoulder even at the earliest time delays might also suggest that the ICT from is in part directly excited. In either case, we would expect a dependence of the relaxation on the excitation wavelength, when different conformers are preferentially excited within the first absorption band. Such wavelength dependence of the ultrafast relaxation probed by two-dimensional electronic spectroscopy has been reported for the PCDTBT polymer, where planar conformations could be preferentially excited at low wavelengths.[20] For CDTBT in DCB, we however observe no differences between the TA dynamics and spectra recorded with 490, 510 and 530 nm excitation (Fig. 4A and S6 in the ESI†). This indicates that it is likely that only the ICT form (with the double-peaked ESA signature) persists at long time delays, and that this form cannot be reached directly from the ground state, but only *via* the less polar precursor.

Finally, the TA spectra of CDTBT in ACN are shown in Fig. 2C. Here, the double-peaked ESA that we assign to the ICT form is again present, as expected for this even more polar solvent. It appears however much faster than that in DCB and only the end of the relaxation process is observed on a sub-picosecond time scale as a red shift of the SE and decay of the initial 820 nm ESA peak. Global analysis yields a time constant of 0.8 ps for the charge transfer relaxation (faster un-resolved components are probable), which confirms that the latter is dependent on solvent reorganization and is faster for low viscosity ACN (Fig. 3C). Indeed, the solvation time of ACN is ultrafast with an inertial 0.09 ps component and a 0.6 ps component.[58] It is interesting to note that the position of the initial ESA band is 845 nm in DEC, 860 nm in DCB and ~820 nm in ACN, thus following a similar trend with refractive index as the steady-state absorption spectrum. The apparent position of the ESA peak might also be influenced by overlap with the nearby SE band, but since both the position and amplitude of the latter depend on solvent polarity, this alone would not explain the correlation of the initial ESA position with refractive

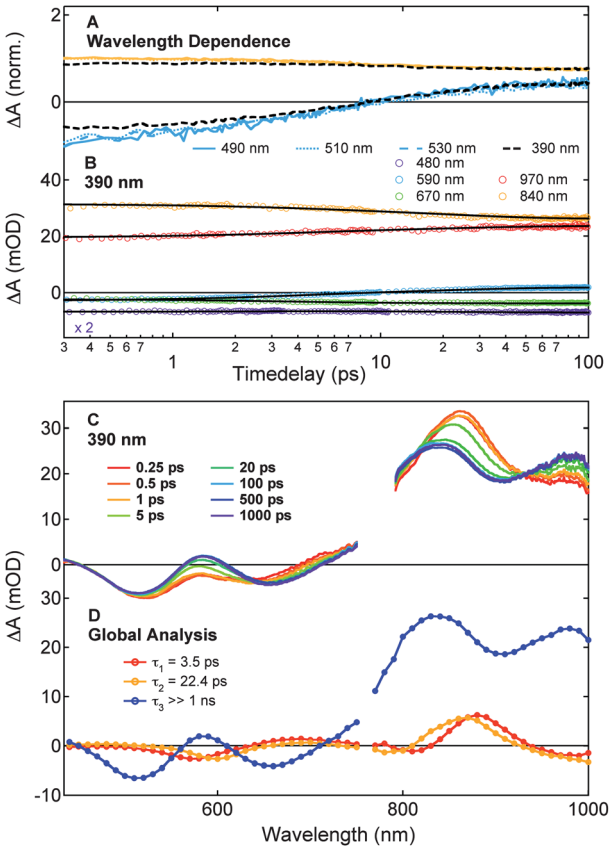

Fig. 4 (A) Transient absorption dynamics of CDTBT in DCB at selected probe wavelengths (590 nm – blue, 840 nm – orange) recorded following excitation at different positions (490 nm, 510 nm, 530 nm, 390 nm) of the first and second absorption bands. Transient absorption dynamics (B) and transient absorption spectra (C) of CDTBT in DCB following 390 nm excitation. Solid black lines are the best global fit. (D) Amplitude spectra associated with the time constants resulting from a multiexponential global analysis of the corresponding transient absorption dynamics.

index. The signature of the ESA after relaxation to the ICT form is also slightly blue-shifted in ACN compared to DCB, but the solvent dependence is very small.

3.2.2 CDTBT in solution (390 nm excitation). When CDTBT in DCB is excited at 390 nm on the red side of the second absorption band, the TA spectra and dynamics shown in Fig. 4B and C are obtained. The similarity to data collected with 510 nm excitation is immediately clear. Thus, internal conversion (IC) is faster than our instrument response and first leads to population of the moderately polar non-relaxed S_1 state, which subsequently relaxes to the long-lived ICT form in the same way as when directly excited. Unlike suggested elsewhere for PCDTBT,[56] the main increase in ICT character in the CDTBT fragment therefore does not occur during IC, but later on. The same time constants of 3.5 ps and 22.4 ps for the charge transfer relaxation in the S_1 state could be used in the global analysis of the 390 nm and 510 nm data, yielding also practically identical decay-associated spectra (Fig. 3B and 4D).

The only measurable difference with 390 nm excitation is a slightly weaker amplitude of the fast components related to spectral relaxation of the SE (590 nm) and ESA (840 nm) with respect to the amplitude of the long-lived spectral signatures (Fig. 4A). The effect is so small that it is only noticeable in the dynamics, but not in the raw TA or amplitude spectra. It might simply be an artifact because different pump pulses are used. Against this speaks the fact that, in contrast to 390 nm excitation, the dynamics recorded when exciting different positions of the first absorption band (with different pulses) are perfectly superposable (Fig. 4A). We tentatively suggest that quite different conformers are generated following IC compared to direct S_1 excitation anywhere in the first band, leading to the small observed difference. Indeed, a recent study of another donor–acceptor copolymer (PCPDTBT) revealed that ultrafast IC occurs only at a particular twist angle of the backbone through a conical intersection, evidencing that IC can influence molecular conformation.[62] For PCDTBT, we have also reported small differences in relaxation of the S_1 state directly excited or populated *via* IC, possibly caused by similar conformation effects.[63]

3.2.3 CDTBT thin film. In the solid state, the electronic environment of CDTBT is no longer determined by a solvent, but by neighboring molecules. Intermolecular interactions and energy transfer between chromophores (excitation hopping) are now possible in the close packed system. The TA spectra of a CDTBT thin film following 510 nm excitation are shown in Fig. 5. The early spectra clearly reveal the GSB and SE, in agreement with the position of our previously reported steady-state spectra.[42] Similar to the observations in polar solvents, there is an evolution within 5 ps from an ESA peaking at 866 nm to a double-peaked feature (860 nm and 955 nm), accompanied by a red shift of the SE. This is very clear in the first two amplitude spectra obtained from multiexponential global analysis of the data (Fig. 5B), which also allows us to assign a 1.2 ps time constant to the process. This finding not only evidences that the environment in the thin film is polar enough to support charge transfer relaxation, but also shows that both the intramolecular and intermolecular rearrangements that make the ICT form accessible are possible and very fast in the solid state. The presumably high polarity in the thin film is somewhat surprising, given the small ground state dipole moment in CDTBT and the generally low dielectric constant of organic semiconductor films. Further investigations to elucidate this are in progress.

While the relaxed excited state in solution shows no further evolution and decays slowly on the nanosecond time scale, the situation in the solid state is very different. Decay of all spectral features including the GSB (mainly with 18.8 ps and 222 ps time constants) demonstrates that CDTBT returns much faster to the ground state in the thin film than in solution (Fig. 5A and S5 of the ESI†). Self-quenching in the solid state is typical of conjugated materials and is for example caused (in somewhat related oligomers) by facilitated excitation hopping to quenching sites.[61] In our case, there is also enhanced ground state recovery due to singlet exciton–exciton annihilation at important concentration of nearby CDTBT excitations, generated in the solid state by the relatively high excitation fluence (90 μJ cm^{-2}) necessary to obtain a clean signal.[64] Indeed, the decay of the ESA slows down when the fluence is halved, mainly because the weights of the 18.8 ps and 222 ps components are reduced (Fig. 5C and D). Apart from causing faster decay of all spectral features, the fluence has no

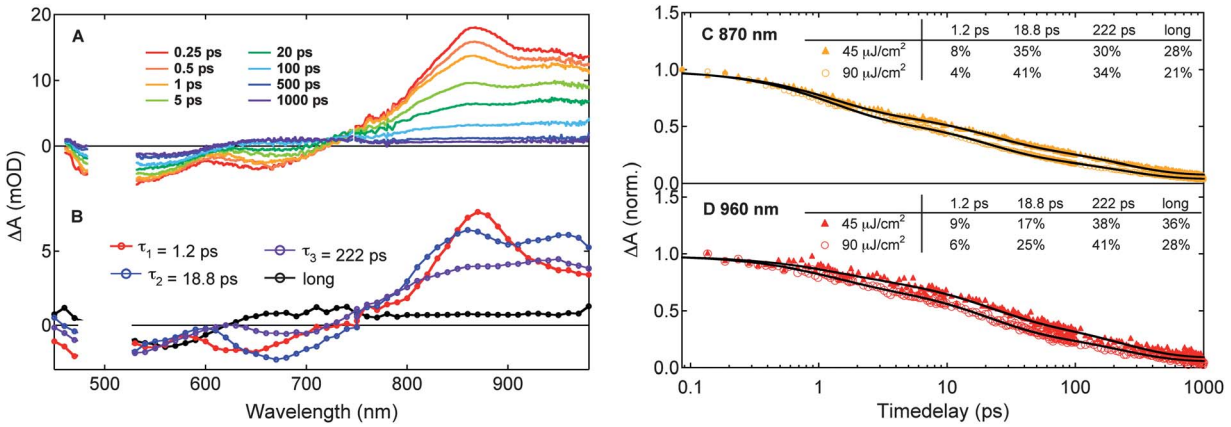

Fig. 5 Transient absorption spectra of a CDTBT thin film, recorded at various time delays following excitation at 510 nm with a fluence of 90 μJ cm^{-2} (A). Corresponding amplitude spectra associated with the time constants resulting from a multiexponential global analysis of the transient absorption dynamics (B). Transient absorption dynamics of a CDTBT thin film recorded at 870 nm (C) and 960 nm (D) as a function of fluence (the inset tables show the results from fits to the data).

effect on the spectral relaxation, *i.e.* the shape of the spectra at a given time delay is identical at the two excitation intensities. We note here that we have not performed a detailed quantitative investigation of the annihilation, which is beyond the scope of the present manuscript and will be addressed in future work. The preliminary multiexponential analysis at only two fluences merely shows that there is an intensity effect because the excitations are no longer isolated in the thin film.

A very interesting observation in the CDTBT thin film is also that there is not simply biexponential decay of the excited state in its ICT form, but that the excited state continues to change its nature. Within tens of picoseconds, the double-peaked ESA signature of the ICT form is replaced by a single broad band centered at 890 nm (very obvious in the amplitude spectrum of the 222 ps component, Fig. 5B). This resembles the ESA signature of a PCDTBT polymer (see below) and might be representative of a more delocalized intermolecular excitation. Moreover, there is complete disappearance of the SE within about 100 ps, although some of the GSB persists (Fig. 5A), indicating population of a non-emitting state (such as the triplet or charge separated state). After about 500 ps, a weak, constant and long-lived signature of this state is the only contribution left in the TA spectra. It is characterized by a slightly red-shifted GSB and a flat positive band extending from 630 nm all the way to 950 nm (end of the measured window).

The red shifted GSB at long time delays can be explained by population of the lowest energy sites after excitation hopping within an inhomogeneous density of states.[61] The flat absorption signature with absent SE resembles the one reported for charge carriers in donor–acceptor conjugated polymers including PCDTBT.[65–67] Its origin is less likely to be the triplet state, since we observed no evidence of intersystem crossing in solution. Nevertheless, we are currently exploring other charge-specific techniques (such as terahertz spectroscopy) to further confirm charge formation in a CDTBT thin film. We suggest that the intermolecular interactions and excited state delocalization in thin film CDTBT might favor splitting of the partial intramolecular charges into completely separate charges on neighboring molecules. Although the CDTBT molecules in the solid state are not covalently linked, the situation reminds of the one recently reported for a series of PTBF donor–acceptor copolymers in solution.[27] Here, separate charges are formed on fragments of the polymer chain (analogue to the CDTBT fragment) from a neutral excited state with ICT character. A small yield of charge carriers in pristine PCDTBT film and other conjugated polymers has also been reported and usually manifests as macroscopic photoconductivity.[42,66,68–71] No photocurrent can be extracted from planar Auston switch devices containing CDTBT, probably due to the poor conduction of the material (no dark current even at high voltage bias).[42]

3.2.4 dTBT in solution. As discussed above, the steady-state spectra of dTBT have a similar solvent-dependence as with CDTBT (only the emission and not the absorption depends on the polarity), but the dipole moment in the relaxed emitting state remains half of that in CDTBT. The TA spectra of dTBT 10 ps after excitation at 490 nm are compared for the three solvents in Fig. 6A. The GSB is seen around 450 nm and a positive signature peaking at 525 nm masks part of the SE, which only appears weakly in the 570 nm region and becomes red shifted with solvent polarity. The most predominant feature is the strong ESA above 600 nm. This band has a sharp peak at 705 nm in DEC, while the peak is slightly shifted to 708 nm in DCB and there is an additional shoulder around 740 nm. In ACN, the peak is broader and blue shifted to 690 nm. The overall solvent-dependent trend of the band position is similar to the one of steady-state absorption and correlates thus with refractive index.

Within the investigated 1 ns window, there is no evolution or decay of the TA features of dTBT in DEC (Fig. S7–9†). The absence of vibrational cooling in the excited state can be explained by the negligible excess energy brought to the system with excitation at 490 nm on the red edge of the absorption spectrum. The excited state in DCB is equally long-lived, but some spectral dynamics (red shift of the SE, rise of the 740 nm shoulder) occur with time constants of 0.13 and 10.8 ps (Fig. 6B and C). Note that the short component is still intermingled with rise of the TA signal within the laser pulse. Even more subtle spectral changes occur with 0.99 ps in ACN (Fig. S7–9†), the faster rate in agreement with the shorter solvation time. The

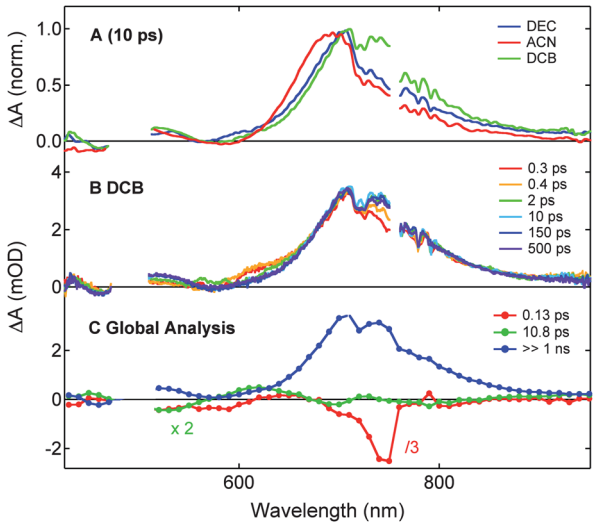

Fig. 6 Transient absorption spectra of dTBT in different solvents at 10 ps time delay (A) and in DCB at various time delays (B) following excitation at 490 nm. Amplitude spectra associated with the time constants resulting from a multi-exponential global analysis of the transient absorption dynamics of dTBT in DCB (C).

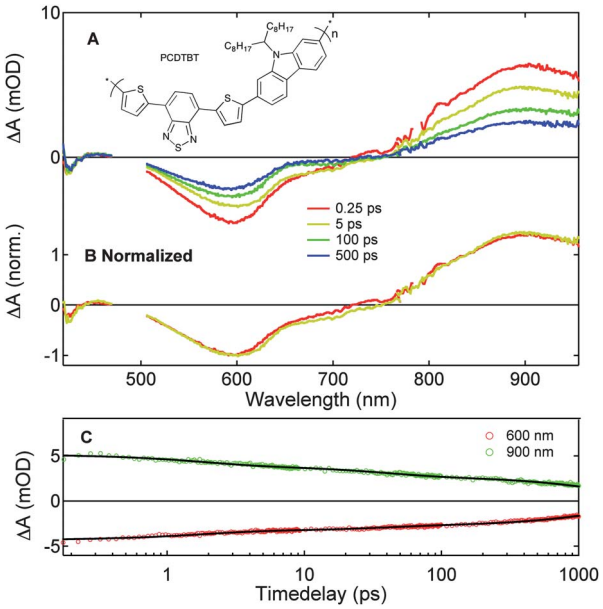

Fig. 7 Transient absorption spectra of PCDTBT (shown in the inset) in DCB at various time delays following excitation at 490 nm, as recorded (A) and normalized (B). Corresponding transient absorption dynamics at selected wavelengths (C); solid black lines are the best global fit.

less pronounced spectral dynamics in dTBT compared to CDTBT point to less significant charge transfer relaxation without the attached carbazole unit, in agreement with the smaller emitting state dipole moment. Apart from energetic considerations, this might be caused by weaker conformational relaxation in the excited state of dTBT. Indeed, the DFT calculation of the excited state geometry (leading to the calculated emission transition in Fig. 1A, in excellent agreement with the experimental spectrum in DEC) shows that the backbone of the molecule is planar in both the ground and excited states (Fig. 1C). Upon relaxation, there is only a marginal contraction of the central benzene ring along the long axis and elongation along the short axis (Fig. S4†).

3.2.5 PCDTBT in solution. The TA spectra of the PCDTBT polymer in DCB following excitation in the first absorption band are shown in Fig. 7A. The GSB signature appears below 440 nm and mainly around 600 nm, while the SE in the 690 nm region is rather weak. The excited state absorbs above 750 nm as a broad band with a maximum at 900 nm (in a similar spectral position as the ICT absorption in CDTBT, but without the double peaked structure, possibly due to more extended delocalization). There is very little evolution of the TA features. A small red shift and increase of the SE occurs within 5 ps (Fig. 7B) due to migration of the photoexcitation to lower energy sites on the polymer chain and some slow conformational rearrangements of the backbone. We could evidence this much more clearly in the time-resolved emission spectra during a polarization-sensitive fluorescence up-conversion study of PCDTBT in solution.[30] The GSB and ESA of the TA spectra decay with time constants of 1.8 ps, 38 ps and 1.8 ns (Fig. 7C), in agreement with the excited state lifetime previously reported with additional short components due to singlet exciton–exciton annihilation.[30,56]

In contrast to CDTBT in the same solvent, there is no sign of charge transfer relaxation in the broad ESA band, although Scholes *et al.* have demonstrated that this indeed occurs in the polymer, when twisted conformations are excited above the bandgap.[20] The increase of dipole moment in the excited state of dissolved PCDTBT is however so fast (less than 200 fs) that it cannot be resolved in our experiments. In the polymer, there is a much higher density of electronic and vibrational states than that in CDTBT, which might explain the ultrafast relaxation. There are also many more torsional degrees of freedom, given additional single bonds linking the repeat units together. While the time scale for charge transfer relaxation for CDTBT in solution is largely determined by solvent rearrangements (see above), intramolecular modes seem to dominate the process in PCDTBT, so that the occurrence of the relaxation largely depends on how twisted the excited polymer chains are.[20] Of course, it must also be taken into account that the environment in dissolved PCDTBT is not only determined by solvent molecules, but also by neighboring chromophores in the (possibly entangled) polymer chain. To bring more insight to the matter, we are planning a future TA investigation of relaxation in PCDTBT as a function of excitation intensity, wavelength and molecular weight.

4 Charge transfer and device applications

Charge transfer transitions and changes in dipole moment during excited state relaxation are issues that have to be seriously considered for all conjugated polymers with a donor–acceptor structure. Nevertheless, they manifest very differently depending on the material. For example, the PBDTTPD donor–acceptor copolymer has planar conformation in both the ground and excited states; so there is no torsional nor charge transfer relaxation and the ICT character in the excited state

remains moderate.[20] On the other hand, ultrafast charge separation within the polymer chain was observed in a series of PTBF copolymers in solution.[27] Even if this charge separation occurred between entire fragments of the PTBF chains and not just between the localized donor and acceptor monomers, it seemed to be favored by stronger local ICT character (*i.e.* a larger difference in electronegativity between the donor and acceptor units). Within the series, a correlation between the yield of intramolecular separate charges in the polymers and the photovoltaic efficiency in corresponding polymer:fullerene bulk heterojunction devices was found, confirming the popular notion that ICT in donor–acceptor copolymers helps splitting of the exciton into free charge carriers for OPV applications.[20,37] We note however that free charge generation in polymer:fullerene blends is also highly efficient in PBDTTPD with moderate ICT character or in P3HT, which is not a donor–acceptor copolymer.[16,72]

A possible reason is that not only the strength of ICT character, but also the extent of wavefunction delocalization in the excited state and in the charges increases the efficiency of OPV devices. Delocalization in the excited state, even if very short-lived before self-localization,[24,25,39–41] allows us to sample a greater spatial extent of the bulk heterojunction and can help to reach a fullerene interface for charge separation on the ultrafast time scale.[29,63,73] Moreover, it was suggested that free charge carriers (as opposed to bound charges across the polymer:fullerene interface) are generated from "hot" delocalized states of the charged species.[28] Device efficiency might therefore suffer in conjugated donor–acceptor copolymers where the ICT character in the excited state is too strong with very localized electron and hole distributions. This might explain why PCDTBT performs better in solar cells compared to related carbazole polymers copolymerized with stronger electron accepting units, although higher efficiency was expected from their energy levels.[37] Given the <200 fs time scale for both charge transfer relaxation in pristine PCDTBT and for charge separation with a fullerene in the bulk heterojunction blend,[20,74] a competition between the two processes is likely. The latter might partly occur from the initially excited, possibly more delocalized non-relaxed S_1 state, rather than after relaxation to the ICT form. In line with this, the photocurrent yield in pristine PCDTBT is higher with excitation in the second than in the first absorption band, which we ascribed to stronger delocalization of the initially excited state, from where charges are formed before relaxation.[42] The HOMO and LUMO levels in the PTBF series are also very delocalized,[27] which might help, together with appropriate ICT character, to form the observed charges in the isolated polymer chains.

Beyond OPV applications, the co-existence of electron rich and electron poor units leads to ambipolar charge transport in organic field effect transistors (OFETs) made of certain conjugated donor–acceptor polymers.[31–33] This property is also useful in OLEDs, where more balanced charge injection and transport have been achieved with donor–acceptor oligomers and polymers.[61,75–78] OLED applications also necessitate high fluorescence quantum yield. We saw here with the CDTBT model oligomer that stabilization of an ICT excited state in a polar medium reduces the emission yield. In the solid state, even weaker fluorescence is expected, since intermolecular interactions favor formation of separate charges. In the development of new donor–acceptor OLED materials, it is therefore important to avoid too pronounced ICT character in the directly as well as relaxed excited state.

5 Conclusions

An important photovoltaic material, conjugated polymer PCDTBT, undergoes ultrafast intramolecular charge transfer relaxation when the excited state is populated by light absorption.[20] This is highly significant for photovoltaic applications, since both the relaxation in the pristine polymer and the charge separation with a fullerene in the bulk heterojunction blend occur on the <200 fs time scale,[20,74] so that the processes can compete. It is possible that the fastest components of the polymer:fullerene charge separation occur from the initially excited, possibly more delocalized S_1 state, rather than from the relaxed excited state with higher ICT character. The ~200 fs time scale associated with the increase of ICT character in pristine PCDTBT, as well as the limited solubility of the polymer in solvents with varying polarity, make it challenging to investigate the details of the relaxation mechanism using for example transient absorption spectroscopy. We show here that those difficulties can be overcome by studying the model compound CDTBT, a fragment of the polymer chain, which represents its repeat unit. Not only is CDTBT soluble in most organic solvents, but relaxation is slowed down in a reduced density of states compared to the polymer.

Similar to the PCDTBT "camel back" absorption spectrum, CDTBT displays two broad, slightly blue shifted, absorption bands in the visible range. Photoexcitation anywhere in the low energy band populates the S_1 state in a non-relaxed form, which has moderate ICT character, in agreement with the lack of correlation of the absorption spectrum with solvent polarity. The non-relaxed S_1 state is also populated *via* ultrafast (<200 fs) internal conversion following absorption in the second band. In polar solvents only, our transient absorption spectra show a subsequent relaxation mechanism leading to an increase of ICT character, to a polarity-dependent emission wavelength and to reduced fluorescence quantum yield. This transition is mainly driven by solvation of the excited state and occurs on a similar solvent-dependent time scale. Additionally, intramolecular relaxation to a more planar conformation most probably plays a role in increasing the intramolecular dipole. Very interestingly, this charge transfer relaxation also occurs in only 1.2 ps in the solid state (CDTBT thin film), showing that the necessary intramolecular and intermolecular rearrangements are possible and that the environment is sufficiently polar. Moreover, there is in this case evidence for intermolecular delocalization and possibly for evolution from the partial intramolecular charges to separate charges between neighboring molecules. They can however not be extracted as photocurrent, due to very low conductivity of the material. Finally, we observed a lesser extent of charge transfer relaxation

in the dTBT fragment (without the carbazole), where conformational changes in the excited state are small and relaxation is determined only by solvation.

There are numerous advantages in using conjugated donor–acceptor materials for organic electronic applications, such as reduced bandgap or ambipolar charge transport. Intramolecular charge transfer states in photoexcited polymers can also act as precursors for free charge carriers in polymer:fullerene bulk heterojunction solar cells. However, if the electron and hole distributions in the excited state become too localized, this can be problematic for OPV functioning. Similarly, too pronounced charge transfer character reduces fluorescence quantum yield for OLED applications. If strong charge transfer character only appears after excited state relaxation, such as in PCDTBT, there can also be competition between functional processes (for example OPV charge carrier generation) and the charge transfer relaxation. When designing conjugated donor–acceptor materials for specific applications, it is therefore imperative to control the extent of charge transfer in the ground and excited states, its interplay with delocalization, and the way it changes during relaxation. Control of torsional conformation and conjugation lengths through introduction of side chains and conjugation breaks provides synthetic means to achieve this.[79,80]

Acknowledgements

We thank Professor Mario Leclerc for providing the building block materials. N.B. thanks the Swiss National Science Foundation for funding through the Ambizione Fellowship PZ00P2_136853, Prof. Jacques Moser for providing the experimental facilities and Dr Robin Humphrey-Baker for use of the Fluorolog. We thank Prof. Alan J. Heeger for providing PCDTBT and for allowing preliminary measurements on his equipment. Prof. Kevin Sivula and Dr Swati De are acknowledged for purification of CDTBT. We thank the NCCR-MUST network of the Swiss National Science Foundation for funding and for promoting collaborative work.

Notes and references

1 X. Zhao and X. Zhan, *Chem. Soc. Rev.*, 2011, **40**, 3728–3743.
2 A. Facchetti, *Chem. Mater.*, 2010, **23**, 733–758.
3 A. J. Heeger, N. S. Sariciftci and E. B. Namdas, *Semiconducting and Metallic Polymers*, Oxford University Press Oxford, UK, 2010.
4 G. Malliaras and R. Friend, *Phys. Today*, 2005, **58**, 53–58.
5 S. R. Forrest, *Nature*, 2004, **428**, 911–918.
6 G. Li, R. Zhu and Y. Yang, *Nat. Photonics*, 2012, **6**, 153–161.
7 L. P. Yu, Y. Y. Liang, Z. Xu, J. B. Xia, S. T. Tsai, Y. Wu, G. Li and C. Ray, *Adv. Mater.*, 2010, **22**, E135–E138.
8 S. H. Park, A. Roy, S. Beaupre, S. Cho, N. Coates, J. S. Moon, D. Moses, M. Leclerc, K. Lee and A. J. Heeger, *Nat. Photonics*, 2009, **3**, 297–302.
9 B. C. Thompson and J. M. J. Frechet, *Angew. Chem., Int. Ed. Engl.*, 2008, **47**, 58–77.
10 G. Yu, J. Gao, J. C. Hummelen, F. Wudl and A. J. Heeger, *Science*, 1995, **270**, 1789–1791.
11 A. Sandström, H. F. Dam, F. C. Krebs and L. Edman, *Nat. Commun.*, 2012, **3**, 1002.
12 S. I. Ahn, W. K. Kim, S. H. Ryu, K. J. Kim, S. E. Lee, S.-H. Kim, J.-C. Park and K. C. Choi, *Org. Electron.*, 2012, **13**, 980–984.
13 S. J. Evenson, M. J. Mumm, K. I. Pokhodnya and S. C. Rasmussen, *Macromolecules*, 2011, **44**, 835–841.
14 M. Saleh, Y.-S. Park, M. Baumgarten, J.-J. Kim and K. Müllen, *Macromol. Rapid Commun.*, 2009, **30**, 1279–1283.
15 M. Gross, D. C. Muller, H.-G. Nothofer, U. Scherf, D. Neher, C. Brauchle and K. Meerholz, *Nature*, 2000, **405**, 661–665.
16 I. A. Howard, R. Mauer, M. Meister and F. Laquai, *J. Am. Chem. Soc.*, 2010, **132**, 14866–14876.
17 I.-W. Hwang, C. Soci, D. Moses, Z. Zhu, D. Waller, R. Gaudiana, C. J. Brabec and A. J. Heeger, *Adv. Mater.*, 2007, **19**, 2307–2312.
18 K. G. Jespersen, F. L. Zhang, A. Gadisa, V. Sundstrom, A. Yartsev and O. Inganas, *Org. Electron.*, 2006, **7**, 235–242.
19 C. J. Brabec, G. Zerza, G. Cerullo, S. De Silvestri, S. Luzzati, J. C. Hummelen and S. Sariciftci, *Chem. Phys. Lett.*, 2001, **340**, 232–236.
20 I. Hwang, S. Beaupre, M. Leclerc and G. D. Scholes, *Chem. Sci.*, 2012, **3**, 2270–2277.
21 P. Parkinson, C. Muller, N. Stingelin, M. B. Johnston and L. M. Herz, *J. Phys. Chem. Lett.*, 2010, **1**, 2788–2792.
22 E. Collini and G. D. Scholes, *Science*, 2009, **323**, 369–373.
23 N. P. Wells, B. W. Boudouris, M. A. Hillmyer and D. A. Blank, *J. Phys. Chem. C*, 2007, **111**, 15404–15414.
24 A. Ruseckas, P. Wood, I. D. W. Samuel, G. R. Webster, W. J. Mitchell, P. L. Burn and V. Sundstrom, *Phys. Rev. B: Condens. Matter Mater. Phys.*, 2005, **72**, 115214.
25 T. E. Dykstra, V. Kovalevskij, X. J. Yang and G. D. Scholes, *Chem. Phys.*, 2005, **318**, 21–32.
26 J. Sperling, F. Milota and H. F. Kauffmann, *Opt. Spectrosc.*, 2005, **98**, 729–739.
27 B. S. Rolczynski, J. M. Szarko, H. J. Son, Y. Y. Liang, L. P. Yu and L. X. Chen, *J. Am. Chem. Soc.*, 2012, **134**, 4142–4152.
28 A. A. Bakulin, A. Rao, V. G. Pavelyev, P. H. M. van Loosdrecht, M. S. Pshenichnikov, D. Niedzialek, J. Cornil, D. Beljonne and R. H. Friend, *Science*, 2012, **335**, 1340–1344.
29 N. Banerji, S. Cowan, E. Vauthey and A. J. Heeger, *J. Phys. Chem. C*, 2011, **115**, 9726–9739.
30 N. Banerji, S. Cowan, M. Leclerc, E. Vauthey and A. J. Heeger, *J. Am. Chem. Soc.*, 2010, **132**, 17459–17470.
31 J. D. Yuen, R. Kumar, D. Zakhidov, J. Seifter, B. Lim, A. J. Heeger and F. Wudl, *Adv. Mater.*, 2011, **23**, 3780–3785.
32 P. Sonar, S. P. Singh, Y. Li, M. S. Soh and A. Dodabalapur, *Adv. Mater.*, 2010, **22**, 5409–5413.
33 J. C. Bijleveld, A. P. Zoombelt, S. G. J. Mathijssen, M. M. Wienk, M. Turbiez, D. M. de Leeuw and R. A. J. Janssen, *J. Am. Chem. Soc.*, 2009, **131**, 16616–16617.
34 E. Bundgaard and F. C. Krebs, *Sol. Energy Mater. Sol. Cells*, 2007, **91**, 954–985.
35 H. A. M. van Mullekom, J. A. J. M. Vekemans, E. E. Havinga and E. W. Meijer, *Mater. Sci. Eng., R*, 2001, **32**, 1–40.

36 A. J. Heeger, Y. M. Sun, C. J. Takacs, S. R. Cowan, J. H. Seo, X. Gong and A. Roy, *Adv. Mater.*, 2011, **23**, 2226–2230.
37 N. Blouin, A. Michaud, D. Gendron, S. Wakim, E. Blair, R. Neagu-Plesu, M. Belletete, G. Durocher, Y. Tao and M. Leclerc, *J. Am. Chem. Soc.*, 2008, **130**, 732–742.
38 N. Blouin, A. Michaud and M. Leclerc, *Adv. Mater.*, 2007, **19**, 2295–2300.
39 N. P. Wells and D. A. Blank, *Phys. Rev. Lett.*, 2008, **100**, 086403.
40 X. J. Yang, T. E. Dykstra and G. D. Scholes, *Phys. Rev. B: Condens. Matter Mater. Phys.*, 2005, **71**, 045203.
41 F. Milota, J. Sperling, A. Tortschanoff, V. Szocs, L. Kuna and H. F. Kauffmann, *J. Lumin.*, 2004, **108**, 205–209.
42 N. Banerji, E. Gagnon, P.-Y. Morgantini, S. Valouch, A. R. Mohebbi, J.-H. Seo, M. Leclerc and A. J. Heeger, *J. Phys. Chem. C*, 2012, **116**, 11456–11469.
43 C. Kitamura, S. Tanaka and Y. Yamashita, *Chem. Mater.*, 1996, **8**, 570–578.
44 N. Banerji, G. Angulo, I. Barabanov and E. Vauthey, *J. Phys. Chem. A*, 2008, **112**, 9665–9674.
45 P. C. Beaumont, D. G. Johnson and B. J. Parsons, *J. Chem. Soc., Faraday Trans.*, 1993, **89**, 4185–4191.
46 M. Peterliska, U. Gossman and E. Gross, *Phys. Rev. Lett.*, 1996, **76**, 1212.
47 M. E. Casida, *Recent Advances in Density Functional Methods*, World Scientific, Singapore, 1995.
48 M. Marques and E. Gross, *Annu. Rev. Phys. Chem.*, 2004, **55**, 4427.
49 Y. Zhao and D. G. Truhlar, *Theor. Chem. Acc.*, 2008, **120**, 215–241.
50 M. J. Frisch, G. W. Trucks, H. B. Schlegel, G. E. Scuseria, M. A. Robb, J. R. Cheeseman, G. Scalmani, V. Barone, B. Mennucci, G. A. Petersson, H. Nakatsuji, M. Caricato, X. Li, H. P. I. Hratchian, A. F. Izmaylov, J. Bloino, G. Zheng, J. L. Sonnenberg, M. Hada, M. Ehara, K. Toyota, R. Fukuda, J. Hasegawa, M. Ishida, T. Nakajima, Y. Honda, O. Kitao, H. Nakai, T. Vreven, J. A. Montgomery, Jr., J. E. Peralta, F. Ogliaro, M. Bearpark, J. J. Heyd, E. Brothers, K. N. Kudin, V. N. Staroverov, R. Kobayashi, J. Normand, K. Raghavachari, A. Rendell, J. C. Burant, S. S. Iyengar, J. Tomasi, M. Cossi, N. Rega, N. J. Millam, M. Klene, J. E. Knox, J. B. Cross, V. Bakken, C. Adamo, J. Jaramillo, R. Gomperts, R. E. Stratmann, O. Yazyev, A. J. Austin, R. Cammi, C. Pomelli, J. W. Ochterski, R. L. Martin, K. Morokuma, V. G. Zakrzewski, G. A. Voth, P. Salvador, J. J. Dannenberg, S. Dapprich, A. D. Daniels, Ö. Farkas, J. B. Foresman, J. V. Ortiz, J. Cioslowski and D. J. Fox, *Gaussian 09, Revision B.01*, Gaussian, Inc., Wallingford CT, 2009.
51 W. Humphrey, A. Dalke and K. Schulten, *J. Mol. Graphics*, 1996, **14**, 33, Visual Molecular Dynamics.
52 C. Risko, M. D. McGehee and J. L. Bredas, *Chem. Sci.*, 2011, **2**, 1200–1218.
53 L. Pandey, C. Doiron, J. S. Sears and J.-L. Brédas, *Phys. Chem. Chem. Phys.*, 2012, **14**, 14243–14248.
54 R. F. Li, J. J. Zheng and D. G. Truhlar, *Phys. Chem. Chem. Phys.*, 2010, **12**, 12697–12701.
55 M. J. G. Peach, P. Benfield, T. Helgaker and D. J. Tozer, *J. Chem. Phys.*, 2008, **128**, 044118.
56 B. Gieseking, B. Jäck, E. Preis, S. Jung, M. Forster, U. Scherf, C. Deibel and V. Dyakonov, *Adv. Energy Mater.*, 2012, **2**, 1477–1482.
57 A. Pigliucci, G. Duvanel, L. M. L. Daku and E. Vauthey, *J. Phys. Chem. A*, 2007, **111**, 6135–6145.
58 M. L. Horng, J. A. Gardecki, A. Papazyan and M. Maroncelli, *J. Phys. Chem.*, 1995, **99**, 17311–17337.
59 Z. R. Grabowski, K. Rotkiewicz and W. Rettig, *Chem. Rev.*, 2003, **103**, 3899–4031.
60 M. M. Martin, P. Plaza, P. Changenet-Barret and A. Siemiarczuk, *J. Phys. Chem. A*, 2002, **106**, 2351–2358.
61 R. Karpicz, S. Puzinas, S. Krotkus, K. Kazlauskas, S. Jursenas, J. V. Grazulevicius, S. Grigalevicius and V. Gulbinas, *J. Chem. Phys.*, 2011, **134**, 204508.
62 D. Fazzi, G. Grancini, M. Maiuri, D. Brida, G. Cerullo and G. Lanzani, *Phys. Chem. Chem. Phys.*, 2012, **14**, 6367–6374.
63 N. Banerji, S. Cowan, M. Leclerc, E. Vauthey and A. J. Heeger, *J. Am. Chem. Soc.*, 2010, **132**, 17459–17470.
64 A. J. Lewis, A. Ruseckas, O. P. M. Gaudin, G. R. Webster, P. L. Burn and I. D. W. Samuel, *Org. Electron.*, 2006, **7**, 452–456.
65 F. Etzold, I. A. Howard, N. Forler, D. M. Cho, M. Meister, H. Mangold, J. Shu, M. R. Hansen, K. Muellen and F. Laquai, *J. Am. Chem. Soc.*, 2012, **134**, 10569–10583.
66 M. H. Tong, N. E. Coates, D. Moses, A. J. Heeger, S. Beaupre and M. Leclerc, *Phys. Rev. B: Condens. Matter Mater. Phys.*, 2010, **81**, 125210.
67 S. De, T. Pascher, M. Maiti, K. G. Jespersen, T. Kesti, F. L. Zhang, O. Inganas, A. Yartsev and V. Sundstrom, *J. Am. Chem. Soc.*, 2007, **129**, 8466–8472.
68 O. G. Reid, J. A. N. Malik, G. Latini, S. Dayal, N. Kopidakis, C. Silva, N. Stingelin and G. Rumbles, *J. Polym. Sci., Part B: Polym. Phys.*, 2012, **50**, 27–37.
69 V. Gulbinas, Y. Zaushitsyn, H. Bassler, A. Yartsev and V. Sundstrom, *Phys. Rev. B: Condens. Matter Mater. Phys.*, 2004, **70**, 035215.
70 C. Silva, A. S. Dhoot, D. M. Russell, M. A. Stevens, A. C. Arias, J. D. MacKenzie, N. C. Greenham, R. H. Friend, S. Setayesh and K. Mullen, *Phys. Rev. B: Condens. Matter Mater. Phys.*, 2001, **64**, 125211.
71 P. B. Miranda, D. Moses and A. J. Heeger, *Phys. Rev. B: Condens. Matter Mater. Phys.*, 2001, **6408**, 081201.
72 A. A. Paraecattil, S. Beaupré, M. Leclerc, J.-E. Moser and N. Banerji, *J. Phys. Chem. Lett.*, 2012, **3**, 2952–2958.
73 S. R. Cowan, N. Banerji, W. L. Leong and A. J. Heeger, *Adv. Funct. Mater.*, 2012, **22**, 1116–1128.
74 F. Etzold, I. A. Howard, R. Mauer, M. Meister, T.-D. Kim, K.-S. Lee, N. S. Baek and F. Laquai, *J. Am. Chem. Soc.*, 2011, **133**, 9469–9479.
75 Y. X. Yang, R. T. Farley, T. T. Steckler, S. H. Eom, J. R. Reynolds, K. S. Schanze and J. G. Xue, *J. Appl. Phys.*, 2009, **106**, 044509.
76 Y. Li, A. Y. Li, B. X. Li, J. Huang, L. Zhao, B. Z. Wang, J. W. Li, X. H. Zhu, J. B. Peng, Y. Cao, D. G. Ma and J. Roncali, *Org. Lett.*, 2009, **11**, 5318–5321.

77 S. T. Huang, D. J. Liaw, L. G. Hsieh, C. C. Chang, M. K. Leung, K. L. Wang, W. T. Chen, K. R. Lee, J. Y. Lai, L. H. Chan and C. T. Chen, *J. Polym. Sci., Part A: Polym. Chem.*, 2009, **47**, 6231–6245.
78 J. M. Hancock, A. P. Gifford, Y. Zhu, Y. Lou and S. A. Jenekhe, *Chem. Mater.*, 2006, **18**, 4924–4932.
79 J. Kim, Y. S. Kwon, W. S. Shin, S.-J. Moon and T. Park, *Macromolecules*, 2011, **44**, 1909–1919.
80 R. H. Friend, P. M. Oberhumer, Y. S. Huang, S. Massip, D. T. James, G. L. Tu, S. Albert-Seifried, D. Beljonne, J. Cornil, J. S. Kim, W. T. S. Huck, N. C. Greenham and J. M. Hodgkiss, *J. Chem. Phys.*, 2011, **134**, 114901.